THE BELL SYSTEM TECHNICAL JOURNAL
Vol. 51, No. 7, September, 1972
Printed in U.S.A.

On the Accuracy of the Depletion Layer Approximation for Charge Coupled Devices

By J. McKENNA and N. L. SCHRYER

(Manuscript received February 28, 1972)

In this paper we examine the accuracy of a variant of the depletion layer approximation as used in the analysis of the electrostatic potential, in the absence of mobile charge, in various charge coupled devices. The approximation is a linearization of the nonlinear potential equations and is important in the numerical solution of two-dimensional problems. A one-dimensional model is solved both exactly and by means of the depletion layer approximation and the two results are compared. We conclude that this variant of the depletion layer approximation is excellent for buried channel devices, and adequate though not as good for surface devices. Some criteria are given which indicate the excellence of the approximation and can be used to estimate errors in two-dimensional calculations.

The purpose of this paper is to discuss the accuracy of a variant of the well known depletion layer approximation[1,2] used in the analysis of the electrostatic potential, in the absence of mobile charge, in various charge coupled devices (CCD's).[3,4] The approximation is a linearization of the nonlinear potential equations and is important in the numerical solution of two-dimensional problems. An application of these results is given in Refs. 5 and 6. We consider a one-dimensional model, which can be solved exactly, and examine in some detail the errors involved in the approximation. This analysis is a generalization of similar results in a previous paper.[1]

Consider a buried channel CCD[7] formed by a first layer, $0 \leqq y \leqq h_1$, of SiO_2 ; a second layer, $h_1 \leqq y \leqq h_2$, of completely ionized p-type Si; and a third layer, $h_2 \leqq y < \infty$, of uniformly doped n-type Si. (See Fig. 1) Then the dimensionless equations governing the potential $\varphi(x, y)$ are

$$\nabla^2\varphi_1(x, y) = 0, \qquad 0 < y < h_1, \tag{1a}$$

$$\nabla^2\varphi_2(x, y) = \sigma(y), \qquad h_1 < y < h_2, \tag{1b}$$

$$\nabla^2\varphi_3(x, y) = \exp(\varphi_2(x, y)) - 1, \qquad h_2 < y < \infty, \tag{1c}$$

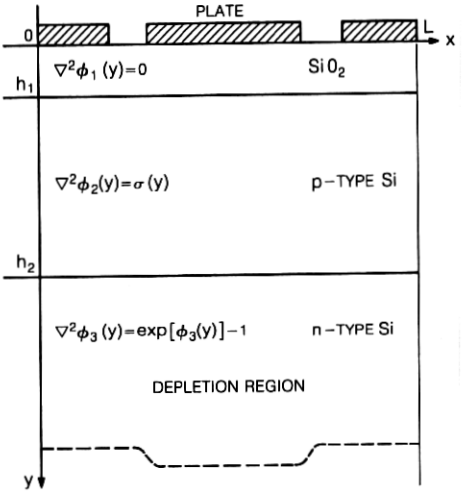

Fig. 1—A schematic diagram of a buried channel CCD.

where $\varphi_j(x, y)$ is the value of $\varphi(x, y)$ in the j-th layer and $\nabla^2 = \partial^2/\partial x^2 + \partial^2/\partial y^2$. In eq. (1), the dimensionless potential $\varphi(x, y)$, and distances, x, y, h_1 , h_2 , are related to the dimensional quantities $\varphi^*(x^*, y^*)$, x^*, y^*, h_1^*, h_2^*, respectively, (measured in MKS units) by

$$\varphi(x, y) = \frac{e}{kT}\varphi^*(x^*, y^*), \tag{2a}$$

$$x = x^*/\lambda_D , \qquad y = y^*/\lambda_D , \qquad h_1 = h_1^*/\lambda_D , \qquad h_2 = h_2^*/\lambda_D , \tag{2b}$$

where the Debye length λ_D is defined by

$$\lambda_D = (\epsilon_2 kT/e^2 N_D^*)^{\frac{1}{2}}, \tag{2c}$$

and $e > 0$ is the electronic charge, k is Boltzmann's constant, T is the absolute temperature, ϵ_2 the permittivity of the Si, and N_D^* is the number density of the donors. Also, the dimensionless density of acceptor ions in the p-layer, $\sigma(y)$, is related to the physical density $N_A^*(y^*)$ by

$$\sigma(y) = N_A^*(y^*)/N_D^* . \tag{2d}$$

We assume that at the boundary $y = 0$, $\varphi_1(x, 0)$ is completely specified.

$$\varphi_1(x, 0) = V_0(x) \leqq 0, \tag{3a}$$

while at the base $y = \infty$,

$$\varphi_3(x, \infty) = 0. \tag{3b}$$

At the internal boundaries, $y = h_1$, $y = h_2$, φ satisfies standard electromagnetic boundary conditions:

$$\varphi_1(x, h_1) = \varphi_2(x, h_1), \qquad \eta \frac{\partial \varphi_1}{\partial y}(x, h_1) = \frac{\partial \varphi_2}{\partial y}(x, h_1) + Q_{ss}, \tag{4a}$$

$$\varphi_2(x, h_2) = \varphi_3(x, h_2), \qquad \frac{\partial \varphi_2}{\partial y}(x, h_2) = \frac{\partial \varphi_2}{\partial y}(x, h_2), \tag{4b}$$

where $\eta = \epsilon_1/\epsilon_2$ is the ratio of the permittivities of SiO_2 to Si, and Q_{ss} is a possible trapped charge at the oxide-semiconductor interface. The remaining boundary condition is taken care of by assuming periodicity in the x-direction

$$\varphi(0, y) = \varphi(L, y), \quad 0 \leqq y < \infty \tag{4c}$$

(see Ref. 5 for a fuller discussion of these boundary conditions).

In the buried channel CCD, the parameters are adjusted so that the potential minimum occurs in layer 2, $h_1 \leqq y \leqq h_2$, where the mobile charges are to be trapped. For most purposes, it is only necessary to know the potential accurately in layer 2. The doping in the p-layer is typically introduced by ion implantation followed by drive in diffusion.[8] Then the acceptor density can be given quite accurately by

$$\sigma(y) = c_s \exp\left\{-\left(\frac{x - h_1}{h_2 - h_1}\right)^2 \ln c_s\right\} - 1 \tag{5}$$

where c_s is the surface density of charge due to the original ion implantation. In some applications it is convenient to replace $\sigma(y)$ by its average

$$\bar{\sigma} = \frac{1}{h_2 - h_1}\int_{h_1}^{h_2} \sigma(y)\, dy = \frac{\sqrt{\pi}}{2}\frac{c_s}{\sqrt{\ln c_s}} \operatorname{erf}(\sqrt{\ln c_s}) - 1, \tag{6}$$

where erf is the error function.[9] In a typical buried channel CCD, region 1, the oxide layer, is 0.1μ thick and $\eta = 1/3$. Region 2, the p-layer is 5μ thick with an initially implanted charge density at the surface of $4.6 \times 10^{15}/\text{cm}^3$, which corresponds to an average doping of $\sim 2 \times 10^{15}/\text{cm}^3$. Region 3, the n-layer, has a doping of $10^{14}/\text{cm}^3$. In our dimensionless units, this corresponds to $h_1 = 0.24$, $h_2 = 12.24$, $c_s = 46$ and $\bar{\sigma} = 19.71$ at room temperature. (In all the examples where $\bar{\sigma}$ is used, we take $\bar{\sigma} = 20$ for simplicity). The potential has been scaled so that 1 volt corresponds to 40 dimensionless units. Typical plate voltages are in the range $-400 \leqq V_0 \leqq 0$. Although we shall

typically assume $Q_{ss} = 0$ in this paper, we include it because it is necessary in some applications.

If layer 2 is removed, we have a surface CCD.[3] In a surface CCD, the mobile charge is trapped at the oxide-semiconductor interface, and only near this interface does the potential need to be known accurately. The remaining dimensions are typically the same as for a buried channel CCD, and the plate voltage is in the range $-400 \leqq V_0 \leqq -160$.

If $\varphi_3(x, h_2)$ is large and negative for $0 \leqq x \leqq L$, then for $y > h_2$ and near h_2, $\exp(\varphi_3(x, y)) \ll 1$ and the equation for φ_3 is approximately $\nabla^2\varphi_3 = -1$. The region where this holds is called the depletion region, and at any point x, the depth of the boundary of this region below $y = h_2$, $R(x)$, is called the depletion depth (see Fig. 1). For (x, y) such that $y > R(x) + h_2$, $|\varphi_3(x, y)| \ll 1$ and we have approximately $\nabla^2\varphi_2 = \varphi_2$. In most problems $R(x)$ is not a constant, but it is nevertheless often a good approximation to replace $R(x)$ by some suitable constant $\hat{R}$. This suggests replacing the system of eqs. (1) by the system of linear equations

$$\nabla^2\psi_1(x, y) = 0, \qquad 0 < y < h_1, \tag{7a}$$

$$\nabla^2\psi_2(x, y) = \sigma(y), \qquad h_1 < y < h_2, \tag{7b}$$

$$\nabla^2\psi_3(x, y) = -1, \qquad h_2 < y < h_3 = h_2 + \hat{R}, \tag{7c}$$

$$\nabla^2\psi_4(x, y) = \psi_4(x, y), \qquad h_3 = h_2 + \hat{R} < y < \infty, \tag{7d}$$

(See Fig. 2). In addition to ψ_1, ψ_2 and ψ_3 satisfying boundary conditions (3a), (4a), (4b) and (4c), we have the boundary conditions

$$\psi_3(x, h_3) = \psi_4(x, h_3), \quad \frac{\partial\psi_3}{\partial y}(x, h_3) = \frac{\partial\psi_4}{\partial y}(x, h_3), \quad \psi_4(x, \infty) = 0 \tag{8}$$

which must hold for $0 \leqq x \leqq L$.

This paper is devoted to studying how the choice of the pseudo-depletion depth $\hat{R}$ affects the accuracy with which $\psi(x, y)$ approximates $\varphi(x, y)$. We do this by considering the special case $V_0(x) \equiv V_0 < 0$, where V_0 is constant, in boundary condition (3a). For this choice of $V_0(x)$, eqs. (1) and (7) reduce to systems of ordinary differential equations the solutions of which are functions of y only. In all that follows, we drop all reference to x, replace ∇^2 by d^2/dy^2 in eqs. (1) and (7), and consider only the one-dimensional problem. The remainder of the paper is devoted to calculating and comparing the values of $\varphi_2(h_2)$ and $\varphi_2'(h_2)$ with $\psi_2(h_2)$ and $\psi_2'(h_2)$, where $' = d/dy$. It is easy to show that for $h_1 \leqq y \leqq h_2$,

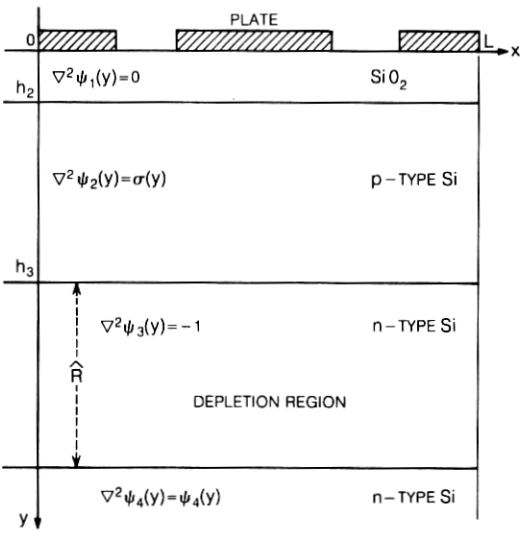

Fig. 2—A schematic diagram of the depletion layer approximation to a one-dimensional, buried channel CCD.

$$| \varphi(y) - \psi(y) | \leqq | \varphi_2(h_2) - \psi_2(h_2) |,$$
$$| \varphi'(y) - \psi'(y) | \leqq | \varphi_2'(h_2) - \psi_2'(h_2) |. \tag{9}$$

We only give the analysis for the buried channel CCD, that is very similar for the surface CCD. We give numerical results for both.

We begin by solving for $\varphi_2(h_2)$ and $\varphi_2'(h_2)$. We can now write

$$\varphi_1(y) = ay + V_0 , \tag{10}$$

$$\varphi_2(y) = \int_y^{h_2} (\xi - y)\sigma(\xi)\, d\xi + b(y - h_2) + c. \tag{11}$$

In addition, a first integral of (1c) subject to (3b) is[1]

$$\tfrac{1}{2}\{\varphi_3'(y)\}^2 = \exp\{\varphi_3(y)\} - \varphi_3(y) - 1. \tag{12}$$

Making use of the boundary conditions (4), it is now easy to show that

$$a = \frac{1}{\eta}\left(b - \int_{h_1}^{h_2} \sigma(\xi)\, d\xi + Q_{ss}\right), \tag{13}$$

$$c = \left(h_2 - h_1 + \frac{h_1}{\eta}\right)b + V_0 + \frac{h_1}{\eta} Q_{ss} - \int_{h_1}^{h_2} \left(\xi - h_1 + \frac{h_1}{\eta}\right)\sigma(\xi)\, d\xi, \tag{14}$$

$$\tfrac{1}{2}b^2 = e^c - c - 1. \tag{15}$$

Equations (14) and (15), for $c = \varphi_2(h_2)$ and $b = \varphi_2'(h_2)$, can be solved numerically. In fact, for most cases of interest $c \ll -1$, so the term e^c in (15) can be neglected, yielding

$$b = \varphi_2'(h_2) = -\left(h_2 - h_1 + \frac{h_1}{\eta}\right) + \sqrt{\left(h_2 - h_1 + \frac{h_1}{\eta}\right)^2 - 2\left[V_0 + 1 - \int_{h_1}^{h_2}\left(\xi - h_1 + \frac{h_1}{\eta}\right)\sigma(\xi)\,d\xi + \frac{h_1}{\eta}Q_{ss}\right]}, \quad (16)$$

$$c = \varphi_2(h_2) = -\tfrac{1}{2}b^2 - 1. \quad (17)$$

It can be shown that for a surface CCD, $\varphi_2'(h_1)$ and $\varphi_2(h_1)$ can be obtained from (16) and (17) by setting $\sigma(y) \equiv 0$ and $h_1 = h_2$.

To solve eqs. (7), we can write

$$\psi_1(y) = Ay + V_0, \qquad 0 \leqq y \leqq h_1, \quad (18a)$$

$$\psi_2(y) = \int_y^{h_2} (\xi - y)\sigma(\xi)\,d\xi + B(y - h_2) + C, \qquad h_1 \leqq y \leqq h_2, \quad (18b)$$

$$\psi_3(y) = -\tfrac{1}{2}(y - h_2)^2 + D(y - h_2) + E, \qquad h_2 \leqq y \leqq h_3, \quad (18c)$$

$$\psi_4(y) = \delta e^{h_2 + \hat{R} - y}, \qquad h_3 = h_2 + \hat{R} \leqq y < \infty, \quad (18d)$$

where the boundary conditions at $y = 0$ and $y = \infty$ have already been used. Upon employing the remaining boundary conditions at $y = h_1$, h_2 and $h_2 + \hat{R} = h_3$, we obtain six equations relating the seven constants A, B, C, D, E, δ and $\hat{R}$.

Our main interest is in cases where $\hat{R}$ is given, so that A, B, C, D, E and δ can be determined in terms of $\hat{R}$. However, we first consider the case where δ is specified. This will provide useful information about picking an optimal value of $\hat{R}$ later on, and will also give a useful criterion for estimating how good the approximate solution is when $\hat{R}$ is specified.

In Ref. (1) the effects of requiring that $\delta = 0$ (the usual depletion layer approximation) or $\delta = -1$ were studied, and it was shown that the choice $\delta = -1$ yields a better approximate solution. It should be noted that requiring $\delta = -1$ is equivalent to requiring that $\psi_3''(h_3) = \psi_4''(h_3)$. We show here that if the value of δ is specified, the choice $\delta = -1$ does yield the best approximation, but the values of $\psi_2(h_2)$ and $\psi_2'(h_2)$ are relatively insensitive to the choice of δ. It is easy to show that in terms of δ,

$$\hat{R} = \delta - \left(h_2 - h_1 + \frac{h_1}{\eta}\right) + \left[\left(h_2 - h_1 + \frac{h_1}{\eta}\right)^2 + \delta^2 + 2\delta - 2V_0 + 2\int_{h_1}^{h_2}\left(\xi - h_1 + \frac{h_1}{\eta}\right)\sigma(\xi)\,d\xi - 2\frac{h_1}{\eta}Q_{ss}\right]^{\frac{1}{2}}, \tag{19a}$$

$$A = \frac{1}{\eta}\hat{R} + \frac{1}{\eta}\left(Q_{ss} - \int_{h_1}^{h_2}\sigma(\xi)\,d\xi - \delta\right), \tag{19b}$$

$$\psi_2'(h_2) = B = D = \hat{R} - \delta, \tag{19c}$$

$$\psi_2(h_2) = C = E = \delta + \hat{R}\delta - \tfrac{1}{2}\hat{R}^2. \tag{19d}$$

For a surface CCD, the expressions for $\psi_2'(h_1)$ and $\psi_2(h_1)$ are given by (19) when $\sigma(y) \equiv 0$ and $h_1 = h_2$.

As a first example, pick the typical parameters mentioned earlier, $h_1 = 0.24$, $h_2 = 12.24$, $Q_{ss} = 0$, $\eta = 1/3$, $V_0 = 0$, and let $\sigma(y) \equiv \bar{\sigma} = 20$. In Fig. 3, using eqs. (16), (17) and (19), we show a plot of

$$e(\psi) = |\,\psi_2(h_2) - \varphi_2(h_2)\,|/|\,\varphi_2(h_2)\,| \tag{20a}$$

and

$$e(\psi') = |\,\psi_2'(h_2) - \varphi_2'(h_2)\,|/|\,\varphi_2'(h_2)\,| \tag{20b}$$

as functions of δ for $-10 \leqq \delta \leqq 10$. It can be shown from (17) that these relative errors have a minimum at $\delta = -1$ (and are even functions

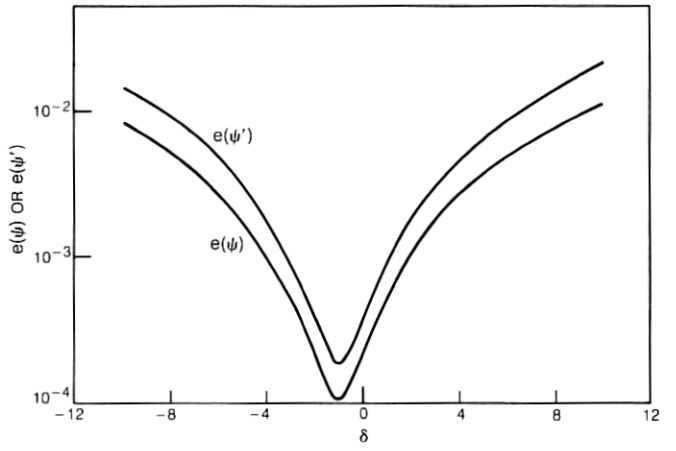

Fig. 3—Plots of $e(\psi)$ and $e(\psi')$ for a buried channel device with $h_1 = 0.24$, $h_2 = 12.24$, $\bar{\sigma} = 20$, $Q_{ss} = 0$, $\eta = \frac{1}{3}$, and $V_0 = 0$ as functions of δ for $-10 \leqq \delta \leqq 10$.

of $\delta + 1$), but over the whole range of δ shown, the maximum relative error in $\psi_2(h_2)$ is only *1.27* percent and in $\psi_2'(h_2)$ is only *2.28* percent.

As a second example, consider a buried channel CCD with the same parameters as in example one, except that in this case we assume that $\sigma(y)$ is given by eq. (5) with $c_s = 46$. In Fig. 4, we show a plot of $e(\psi)$ for this case as a function of δ for $-10 \leqq \delta \leqq 10$. The results are qualitatively the same as in the first example, except that the relative error is about twice as large. It should be remarked that the potential distributions in the first and second examples are quite different. The potential minimum in example one occurs much nearer the bottom of the p-layer than in example two. In example one, $\varphi(h_2) = -1034.5$ while in example two, $\varphi(h_2) = -530.6$, so we would expect the depletion layer approximation to be better in example one than in example two, as it is.

As a third example, consider a surface CCD with $h_1 = h_2 = 0.24$, $\sigma = 0$, $Q_{ss} = 0$, $\eta = 1/3$, and $V_0 = -160$. In Figs. 5a and 5b, using eqs. (16), (17) and (19), we again show plots of $e(\psi)$ and $e(\psi')$ as functions of δ over $-10 \leqq \delta \leqq 10$. We see a maximum relative error of *1.53* percent in $\psi_2(h_1)$ and *18.3* percent in $\psi_2'(h_1)$.

Since the approximation is based on the assumption that $\varphi(h_2)$ is large and negative, the magnitude of $\varphi(h_2)$ must affect the accuracy of the approximation. For the buried channel CCD, $\varphi(h_2)$ is $\lesssim -500$ for all $V_0 \leqq 0$, so in this case, the approximation is very accurate for

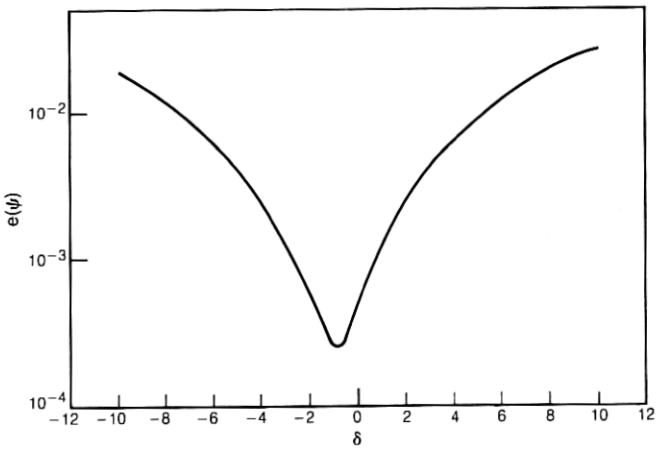

Fig. 4—Plot of $e(\psi)$ for a buried channel device with $h_1 = 0.24$, $h_2 = 12.24$, $c_s = 46$, $Q_{ss} = 0$, $\eta = \frac{1}{3}$, and $V_0 = 0$ as a function of δ for $-10 \leqq \delta \leqq 10$.

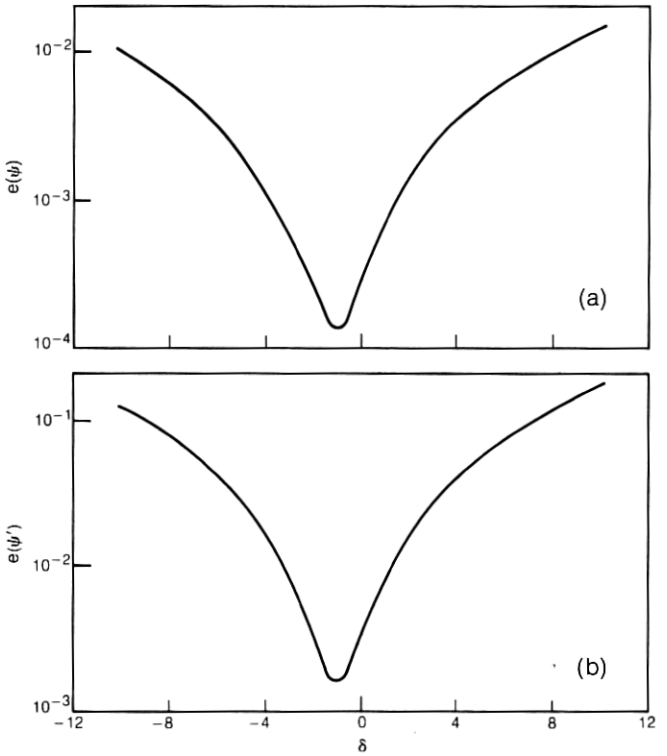

Fig. 5(a) and 5(b)—Plots of $e(\psi)$ and $e(\psi')$, respectively, for a surface device with $h_1 = h_2 = 0.24$, $\sigma = 0$, $Q_{ss} = 0$, $\eta = \frac{1}{3}$ and $V_0 = -160$ as functions of σ for $-10 \leqq \delta \leqq 10$.

any negative V_0 . However, in the surface CCD, as $V_0 \to 0$ we have $\varphi(h_1) \to 0$. Thus for "small" V_0 , we expect the approximation to be quite bad. Figure 6 gives a plot of the relative error $e(\psi)$ for a surface CCD as a function of V_0 using the same parameters as given for Fig. 5 and $\delta = -10$. To maintain an error of the order of 1 percent for all $\delta \in [-10, 10]$, it is clearly necessary to keep $V_0 \leqq -160$.

We turn now to the main problem where $\hat{R}$ is arbitrarily specified. This occurs typically in the numerical solution of two-dimensional problems where it can be reasonably assumed that the depletion depth $R(x)$ does not vary too much with the various plate potentials. Then an average depletion depth is estimated, say from eq. (19a) by setting $\delta = -1$ and choosing for V_0 some average plate potential.

We now investigate the errors involved in this approximation. If

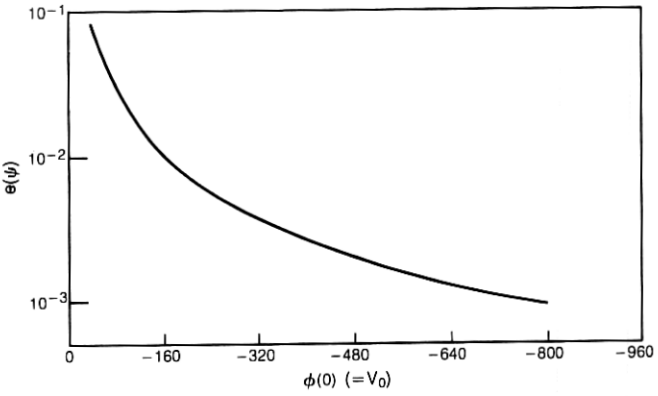

Fig. 6—A plot of $e(\psi)$ for a surface device with $h_1 = h_2 = 0.24$, $\sigma = 0$, $Q_{ss} = 0$, $\eta = \frac{1}{3}$ and $\delta = -10$ as a function of V_0 for $-800 \leqq V_0 \leqq -40$.

$\hat{R}$ is given, then it is easy to show that

$$\psi_2'(h_2) = B = D = \left[\int_{h_1}^{h_2} \left(\xi - h_1 + \frac{h_1}{\eta}\right)\sigma(\xi)\, d\xi - \frac{h_1}{\eta} Q_{ss} - V_0 + \tfrac{1}{2}\hat{R}^2 + \hat{R}\right] \Big/ \left[\hat{R} + 1 + h_2 - h_1 + \frac{h_1}{\eta}\right], \tag{21a}$$

$$A = \frac{1}{\eta}\left(B - \int_{h_1}^{h_2} \sigma(\xi)\, d\xi + Q_{ss}\right), \tag{21b}$$

$$\psi_2(h_2) = C = E = \tfrac{1}{2}\hat{R}^2 + \hat{R} - (\hat{R} + 1)B, \tag{21c}$$

$$\delta = \hat{R} - B. \tag{21d}$$

As before, the above expressions give $\psi_2(h_1)$ and $\psi_2'(h_1)$ for a surface device when we set $\sigma = 0$ and $h_1 = h_2$.

As a fourth example, we consider a buried channel CCD with $h_1 = 0.24$, $h_2 = 12.24$, $\sigma(y) \equiv \bar{\sigma} = 20$, $Q_{ss} = 0$, $\eta = \frac{1}{3}$, and we choose $\hat{R} = 50.98$. From (19a), this corresponds to the "true" depletion depth R (with $\delta = -1$) for a plate voltage $V_0 = -400$. In Fig. 7, using eqs. (16), (17) and (21), we give plots of $e(\psi)$ and $e(\psi')$ as functions of V_0 for $-800 \leqq V_0 \leqq 0$. In Fig. 8, we give a plot of δ as a function of V_0 from (21d) for the same data, and a plot of the "true" value of R from (19a) for $\delta = -1$ as a function of V_0. Several important conclusions can be drawn from these graphs. First, over $-800 \leqq V_0 \leqq 0$, $\psi(y)$ is an excellent approximation to $\varphi(y)$ for $h_1 \leqq y \leqq h_2$, the maximum relative errors in $\psi_2(h_2)$ and $\psi_2'(h_2)$, which occur at $V_0 = 0$, being

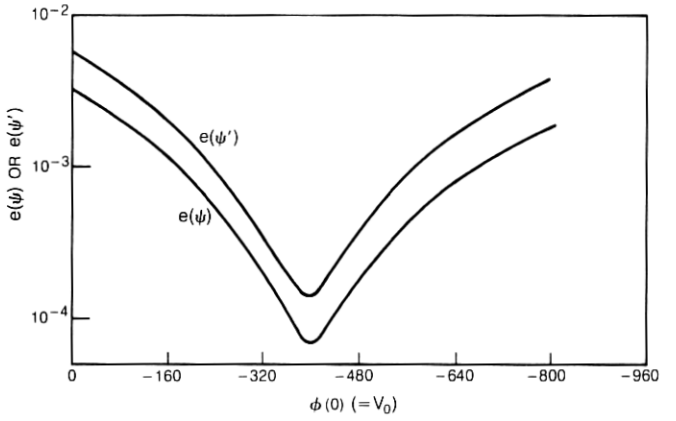

Fig. 7—Plots of $e(\psi)$ and $e(\psi')$ for a buried channel device with $h_1 = 0.24$, $h_2 = 12.24$, $\bar{\sigma} = 20$, $Q_{ss} = 0$, $\eta = \frac{1}{3}$ and $\hat{R} = 50.98$ as functions of V_0 for $-800 \leqq V_0 \leqq 0$.

0.41 percent and 0.74 percent respectively. Second, $\psi(y)$ approximates $\varphi(y)$ excellently over $h_1 \leqq y \leqq h_2$, even though a relatively large error has been made in estimating the true value of R. In fact, $\hat{R} = 50.98$ differs from the "true" value by *11.6* percent at $V_0 = -800$ and by

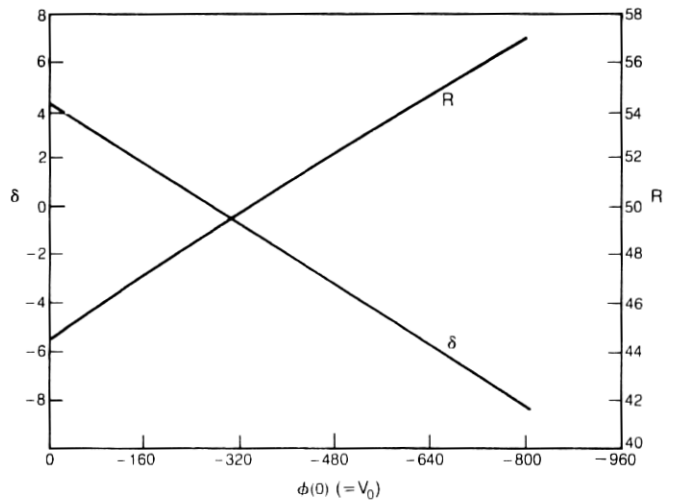

Fig. 8—Plots of δ and "true" R for a buried channel device with $h_1 = 0.24$, $h_2 = 12.24$, $\bar{\sigma} = 20$, $Q_{ss} = 0$, $\eta = \frac{1}{3}$ and $\hat{R} = 50.98$ as functions of V_0 for $-800 \leqq V_0 \leqq 0$.

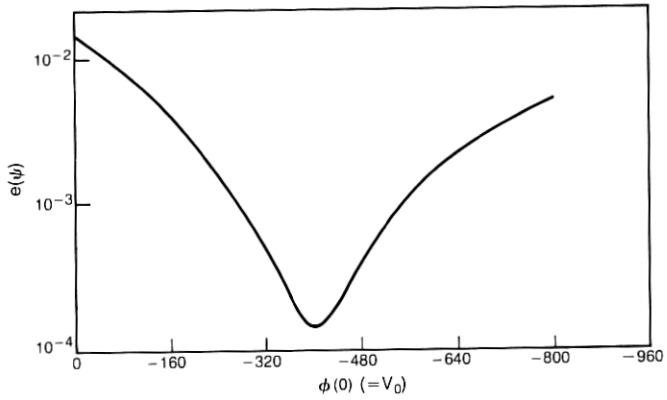

Fig. 9—Plot of $e(\psi)$ for a buried channel device with $h_1 = 0.24$, $h_2 = 12.24$, $c_s = 46$, $Q_{ss} = 0$, $\eta = \frac{1}{3}$ and $\hat{R} = 39.66$ as a function of V_0 for $-800 \leqq V_0 \leqq 0$.

12.7 percent at $V_0 = 0$. Finally, an estimate of the error in $\psi(h_2)$ can be obtained from monitoring δ. For $V_0 \leqq 0$, as long as $-7 \leqq \delta \leqq 5$, the error in $\psi_2(h_2)$ and $\psi_2'(h_2)$ is less than 1 percent.

Next, consider a buried channel CCD with $h_1 = 0.24$, $h_2 = 12.24$,

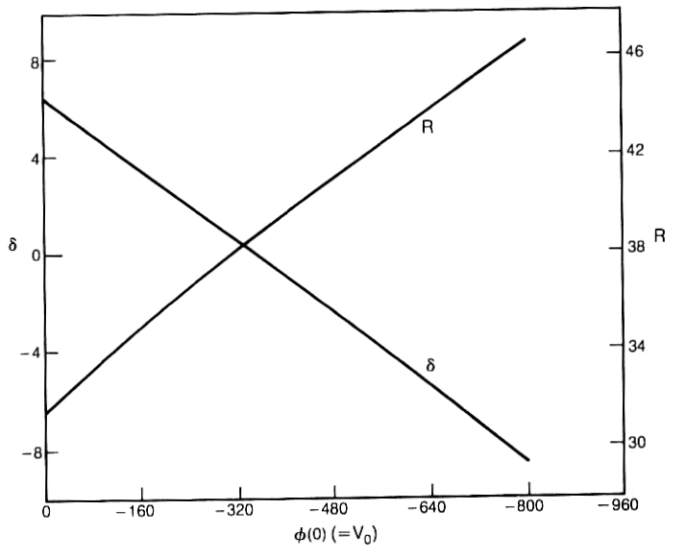

Fig. 10—Plots of δ and "true" R for a buried channel device with $h_1 = 0.24$, $h_2 = 12.24$, $c_s = 46$, $Q_{ss} = 0$, $\eta = \frac{1}{3}$ and $\hat{R} = 39.66$ as functions of V_0 for $-800 \leqq V_0 \leqq 0$.

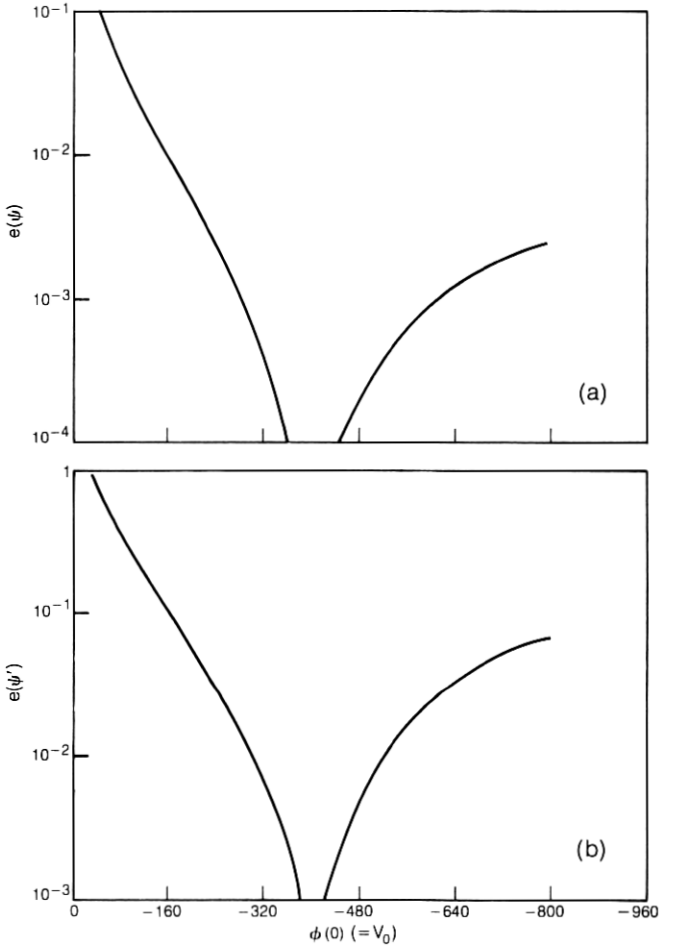

Fig. 11(a) and 11(b)—Plots of $e(\psi)$ and $e(\psi')$, respectively, for a surface device with $h_1 = h_2 = 0.24$, $\sigma = 0$, $Q_{ss} = 0$, $\eta = \frac{1}{3}$ and $\hat{R} = 26.55$ as functions of V_0 for $-800 \leqq V_0 \leqq -40$.

$Q_{ss} = 0$, $\eta = \frac{1}{3}$, with $\sigma(y)$ given by (5) with $c_s = 46$, and with $\hat{R} = 39.66$. From (19a), this corresponds to a "true" value of R (with $\delta = -1$) for a plate voltage of $V_0 = -400$. In Fig. 9, we plot $e(\psi)$ as a function of V_0 for $-800 \leqq V_0 \leqq 0$. In Fig. 10, we give a plot of δ as a function of V_0 from (21d) for the same data, and a plot of the "true" value of R from (19a) for $\delta = -1$ as a function of V_0. The results are qualitatively

the same as for example four, but as we should expect, the errors in using the depletion layer approximation are greater in example five than in example four.

As a final example, we consider a surface CCD with $h_1 = h_2 = 0.24$, $\sigma = 0$, $Q_{ss} = 0$, $\eta = \frac{1}{3}$ and $\hat{R} = 26.55$. From (19a), this corresponds to a "true" value of R (with $\delta = -1$) for a plate voltage of $V_0 = -400$. In Figs. 11a and 11b, using eqs. (16), (17) and (21), we give plots of $e(\psi)$ and $e(\psi')$ as functions of V_0 for $-800 \leqq V_0 \leqq -40$. In Fig. 12, we give a plot of δ as a function of V_0 from (21d) for the same data, and a plot of the "true" value of R from (19a) (for $\delta = -1$) as a function of V_0 . Hence, we note that over the range $-800 \leqq V_0 \leqq -160$, the error in $\psi_2(h_1)$ remains remarkably small, less than 1 percent. However, $\psi_2'(h_1)$ does not approximate $\varphi_2'(h_1)$ nearly as well, especially as $V_0 \to 0$. Note also that in this case much larger errors have been made in estimating R, the error being 39 percent at $V_0 = -160$ and 44.2 percent at $V_0 = -800$. Again, δ provides a check on the accuracy of the approximation, with $-10 \leqq \delta \leqq 8$ assuring an error of less than 1 percent in approximating $\varphi(y)$ in $h_1 \leqq y \leqq h_2$.

We can conclude that this variant of depletion layer approximation works excellently for the buried channel devices in providing approximations to $\varphi(y)$ and $\varphi'(y)$ in the region $h_1 \leqq y \leqq h_2$. In addition, the parameter δ is a good index of the excellence of the approximation. If in a two-dimensional calculation this variant of the depletion layer

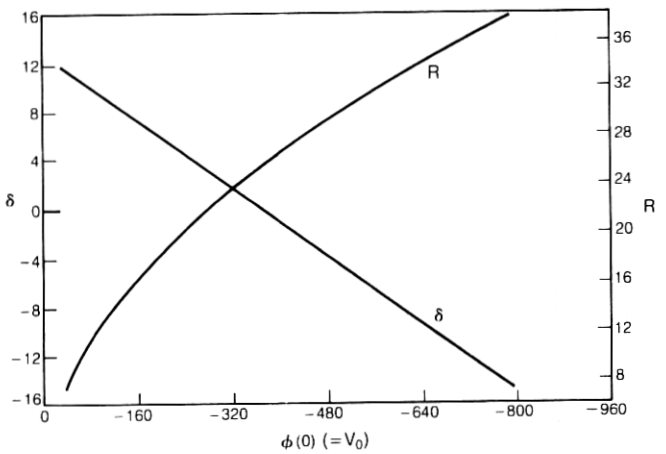

Fig. 12—Plots of δ and "true" R for a surface device with $h_1 = h_2 = 0.24$, $\sigma = 0$, $Q_{ss} = 0$, $\eta = \frac{1}{3}$ and $\hat{R} = 26.55$ as functions of V_0 for $-800 \leqq V_0 \leqq -40$.

approximation is used, then a value of the pseudo-depletion depth $\hat{R}$ is estimated, say from using an average plate potential in eq. (19a). Then, so long as the solution of this approximate problem remains in the interval $[-10, 10]$ along the line $y = \hat{R} + h_2$, one can feel reasonably confident that the approximate solution differs from the true solution, in the region of interest, by at most a few percent. It should be noted that the depletion layer approximation is poor near $y = h_2 + \hat{R}$, but in many important cases this is unimportant. Finally, for surface CCDs, the approximation is good to $\varphi(y)$ but not as good to $\varphi'(y)$.

REFERENCES

1. Lewis, J. A., McKenna, J., and Wasserstrom, E., "Field of Negative Point, Line or Plane Charges in an n-Type Semiconductor," J. Appl. Phys., *41*, No. 10 (September 1970), pp. 4182–4189.
2. For a list of many different treatments of the one-dimensional, nonlinear problem treated here, see: Macdonald, J. R., "Distribution of Space Charge in Homogeneous Metal Oxide Films and Semiconductors," J. Chem. Phys., *40*, No. 12 (June 1964), pp. 3735–3737.
3. Boyle, W. S., and Smith, G. E., "Charged Coupled Semi-conductor Devices," B.S.T.J., *49*, No. 4 (April 1970), pp. 587–593.
4. Amelio, G. F., Tompsett, M. R., and Smith, G. E., "Experimental Verification of Charge Coupled Devices," B.S.T.J., *49*, No. 4 (April 1970), pp. 593–600.
5. McKenna, J., and Schryer, N. L., unpublished work.
6. McKenna, J. and Schryer, N. L., unpublished work.
7. Walden, R. H., Krambeck, R. H., Strain, R. J., McKenna, J., Schryer, N. L., and Smith, G. E., "A Buried Channel Charge Coupled Device," B.S.T.J., this issue, pp. 1635–1640.
8. Grove, A. S., *Physics and Technology of Semiconductor Devices*, John Wiley, New York: John Wiley, 1967, p. 49.
9. Abramowitz, M., and Stegun, J. A., *Handbook of Mathematical Functions*, Washington, D. C.: National Bureau of Standards, 1964, p. 297.